ARTICLE

Phase Transition Behaviour of VO_2 Nanorods

Ying Luo[a], Ming Li[a], Guang-hai Li[a,b*]

a. Key Laboratory of Materials Physics, Anhui Key Laboratory of Nanomaterials and Nanotechnology, Institute of Solid State Physics, Chinese Academy of Sciences, Hefei 230031, China
b. University of Science and Technology of China, Hefei 230026, China

(Dated: Received on April 24, 2014; Accepted on May 15, 2013)

The metal-insulator transition (MIT) of VO_2(M) nanorods was studied. It was found that there were two MITs in the differential scanning calorimetry (DSC) curves of the VO_2(M) nanorods, one situated at low temperature from −3 °C to 19 °C and the other was at high temperature of 65−74 °C. The low temperature MIT was always accompanied with VO_2(B) nanorods, and the high temperature MIT existed singly only in pure VO_2(M) nanorods. The mechanisms of these two MITs were analyzed and discussed.

Key words: Vanadium dioxide, Nanorod, Metal-insulator transition

I. INTRODUCTION

Vanadium dioxide has been regarded as a typical example possessing metal-insulator phase transition (MIT, VO_2(M)↔VO_2(R)). The MIT is fully reversible and can lead to a dramatic change in electrical and optical properties. VO_2(M) is thus regarded as an attractive candidate for a variety of technological applications such as smart thermochromic windows [1], electrical and infrared light switching devices [2, 3], storage media [4] to temperature-sensing devices [5−7].

A number of approaches have been reported for the preparation of VO_2(M) nanomaterials, such as reduction-hydrolysis [8], evaporative decomposition synthesis [9], thermolysis method [10−12], and hydrothermal synthesis [13−17]. Hydrothermal synthesis is a commonly used method to prepare VO_2(M) nanomaterials, and it has been found that if the hydrothermal reaction temperature is not high enough and/or the reaction time is not long enough, one of metastables phases of vanadium dioxides, VO_2(B) instead of VO_2(M) phase will be obtained. In generally, subsequently annealing treatment is needed to obtain VO_2(M) phase.

Many factors are known to affect the MIT of VO_2(M), such as microstructure, defects, particle sizes, grain boundaries and/or interfaces [18−23]. In this work, we report the phase transition of VO_2(M) nanorods. We find that there are two MITs in the DSC curves in the mixed phase of VO_2(B) and VO_2(M) and, one is at low temperature from −3 °C to 19 °C and the other is at high temperature within 65−74 °C.

*Author to whom correspondence should be addressed. E-mail: ghli@issp.ac.cn

II. EXPERIMENTS

VO_2(B) nanorods were synthesized by hydrothermal method. For a typical procedure, 3 g V_2O_5 and 1.82 g oxalic acid ($H_2C_2O_4{\cdot}2H_2O$) were mixed in 50 mL deionized water with stirring at 60 °C in the oil bath for 12 h, and then the mixture was transferred into an autoclave (60 mL) followed by hydrothermal treatment at 220 °C for 48 h. The black precipitate was collected after cooling naturally to room temperature, washed three times using deionized water and alcohol alternatively, and then dried at 80 °C for 12 h. The as-prepared samples were then annealed at 350−550 °C for different time in a nitrogen atmosphere.

The microstructure of the samples was determined by X-ray diffraction (XRD, Philips X'Pert Pro MPD and Cu Kα radiation at 1.54056 Å) and field-emission scanning electron microscopy (FESEM, Sirion 200 operating with an accelerating voltage of 10 kV). The phase transition behavior was analyzed by differential scanning calorimetry (DSC, Netzsch DSC-4000) at a temperature ramp rate of 5 °C/min within the −15 °C to +100 °C range in a flowing nitrogen atmosphere.

III. RESULTS AND DISCUSSION

Figure 1 shows the XRD patterns of the as-prepared and annealed samples. The strong diffraction peaks of the as-prepared sample (Fig.1(a)) can be readily indexed to monoclinic VO_2(B) phase (JCPDS No.01-81-2392), and no peaks related to other vanadium dioxides were observed, indicating the high purity of the VO_2(B) phase. When annealed at 350 °C (Fig.1(b)), the diffraction peaks still belong to VO_2(B) phase, and the XRD peaks related to the VO_2(M) phase are invisible. When annealed at 400 C, a weak peak belonging to the VO_2(M) phase at 2θ=27.9° appears (Fig.1(c)).

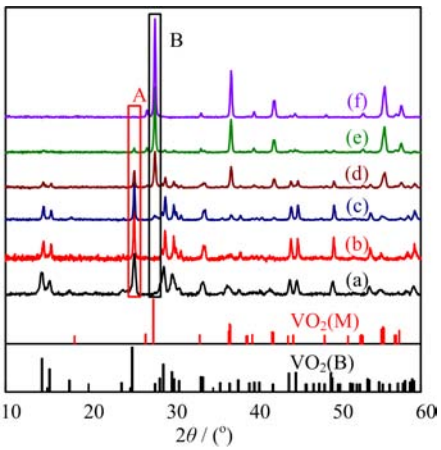

FIG. 1 XRD patterns of as-prepared (a) and annealed samples at (b) 350 °C, (c) 400 °C, (d) 450 °C, (e) 500 °C, and (f) 550 °C for 1 h.

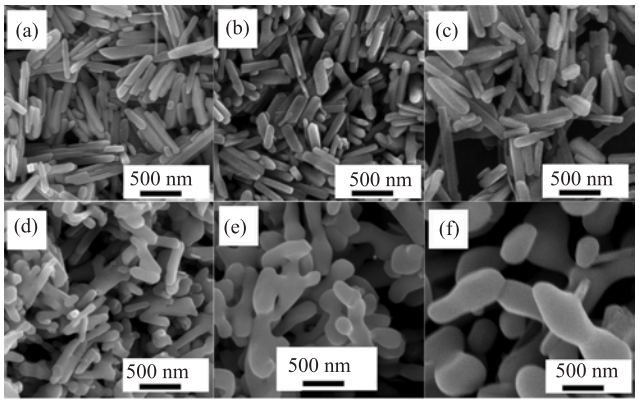

FIG. 2 SEM images of as prepared (a) and annealed samples at (b) 350 °C, (c) 400 °C, (d) 450 °C, (e) 500 °C, and (f) 550 °C for 1 h.

With increasing annealing temperature the number of diffraction peaks and peak intensities belonging to the VO_2(M) phase gradually increase while that belonging to VO_2(B) gradually decrease, indicating an increased content of VO_2(M) phase in the annealed samples (Fig.1 (d) and (e)). Finally as the annealing temperature is increased to 550 °C, the characteristic peaks belonging to VO_2(B) phase disappear, and all the diffraction peaks can be indexed to monoclinic VO_2(M) (JCPDS card No.03-65-2358), as shown in Fig.1(f). The rectangle areas marked A and B of Fig.1 indicate that the VO_2(B) has completely transformed to VO_2(M) phase.

Figure 2 shows SEM images of the as-prepared and annealed samples. One can see that the as-prepared VO_2(B) has a rodlike shape with lengths up to several hundred nanometers and typically 40−90 nm in width, as shown in Fig.2(a). It is worth noting that the VO_2(B) nanorods have a uniform thickness and sharp tips. When annealed at 550 °C, VO_2(B) nanorods completely transforms to VO_2(M) nanorods with uneven in thickness and round tips, as shown in Fig.2(f). The sample annealed at 350 °C has the same morphology as the as-prepared sample, indicating that it is still a VO_2(B) phase, as shown in Fig.2(b). From Fig.2 (c)−(e) one can see that the content of the nanorods with an uneven thickness increases with increasing annealing temperature, indicating more VO_2(B) nanorods have transformed to VO_2(M) nanorods, which is in accordance with the above XRD results.

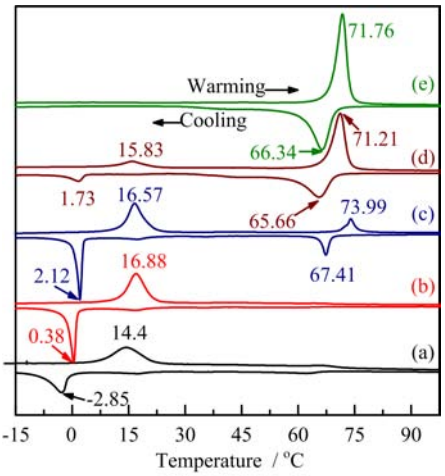

FIG. 3 DSC curves annealed samples at temperature of (a) 350 °C, (b) 400 °C, (c) 450 °C, (d) 500 °C and (e) 550 °C for 1 h.

Figure 3 shows the DSC curves of the samples annealed at different temperatures. One can see that there is only one pair of endothermic and exothermic peaks situated at low temperature when annealed at 350 °C, and the exothermic peak is at about −2.85 °C and the endothermic is at 14.4 °C (Fig.3(a)). With increasing annealing temperature to 400 °C, there is still one pair of endothermic and exothermic peaks with slightly increased peak temperature, as shown in Fig.3(b). As annealing temperature is increased to 450 °C, there are two pairs of endothermic and exothermic peaks, one is situated at low temperature, and the other is at high temperature. The peak temperature of the endothermic and exothermic peaks at high temperature is at 73.99 and 64.41 °C, respectively, as shown in Fig.3(c), which is close to the value for bulk VO_2(M). At annealing temperature of 500 °C, there are still two pairs of endothermic and exothermic peaks, and the endothermic and exothermic peaks at low temperature become much weaker while that at high temperature becomes stronger, as shown in Fig.3(d). At annealing temperature of 550 °C, only one pair of endothermic and exothermic peaks situated at high temperature can be observed, Fig.3(e). The endothermic and exothermic peaks intensities at low temperature firstly slightly increase and then decrease with increasing annealing temperature and finally drop to zero at annealing temperature of 550 °C, while that at high temper-

DOI:10.1063/1674-0068/27/04/471-474

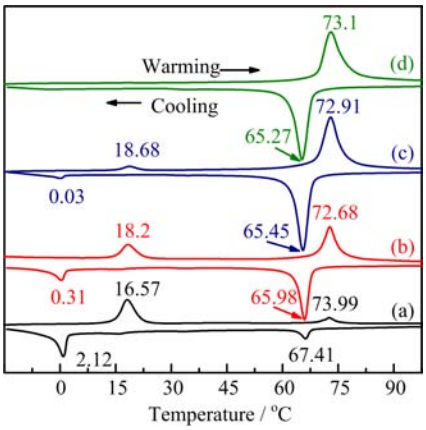

FIG. 4 DSC curves of annealed samples at temperature of 450 °C for (a) 1 h, (b) 2 h, (c) 4 h, and (d) 6 h.

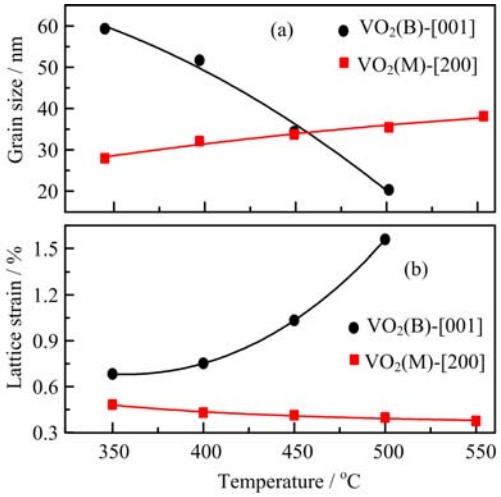

FIG. 5 (a) Grain size and (b) lattice strain of VO_2(B) and VO_2(M) phases for the samples annealed at different temperatures.

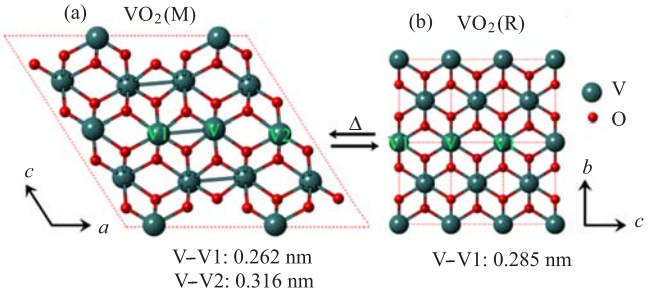

FIG. 6 Crystalline structures of (a) VO_2(M) and (b) VO_2(R). The atomic positions, cell parameters and V−V bonds are taken from Ref.[2] in drawing the crystal structures.

ature always increases with increasing annealing temperature. It is also found that with further increasing annealing temperature to over 550 °C, there is still one pair of endothermic and exothermic peaks situated at high temperature. Combined with XRD analysis, one can see that the endothermic and exothermic peaks at low temperature is always accompanied with VO_2(B) nanorods even without the formation of the VO_2(M) phase (Fig.3(a)), while the endothermic and exothermic peaks at high temperature appear with the formation of the VO_2(M) phase (Fig.3(c)). There is only one pair endothermic and exothermic peaks for pure VO_2(M) nanorods, as shown in Fig.3(e). The same phenomena can also be observed with increasing annealing time, as shown in Fig.4, in which the endothermic and exothermic peaks intensities at low temperature decrease and finally drop to zero with increasing annealing time, and that at high temperature continuously increase with increasing annealing time. From these results, we can conclude that these two pairs of endothermic and exothermic peaks are original from the reversible MIT, and that at high temperature is caused by the VO_2(M) nanorods with a relative large size, while that at low temperature is considered due to the small VO_2(M) crystals closely related to VO_2(B) phase.

From the full width at half maximum (FWHM) of the diffraction peaks marked A and B shown in Fig.1, we can calculate the grain size and lattice strain of VO_2(B) and VO_2(M) phases along the orientation of [001] and [200] in the annealed samples, respectively, and the calculated result is shown in Fig.5. One can see that the grain size of the VO_2(B) nanorods decreases from 59.3 nm to 20.3 nm, and finally to zero, while that of the VO_2(M) nanorods increases from zero to 27.9 nm and finally to 38.1 nm, as shown in Fig.5(a), demonstrating a gradual growth of the VO_2(M) nanorods. The lattice strain of the VO_2(B) nanorods continuously increases, while that of the VO_2(M) nanorods slightly decreases, as shown in Fig.5(b), indicating that the VO_2(R) grains (or VO_2(M) below MIT temperatures) are in a strain environment of VO_2(B) nanorods. The increased lattice strain in the VO_2(B) nanorods might be due to the rearrangement and reshuffling of the octahedra in VO_2(B) phase [2].

The transition from low temperature VO_2(M) metal phase to high temperature VO_2(R) semiconductor phase is fully reversible, and above MIT temperature the VO_2(R) has a tetragonal structure and corresponds to a relatively isotropic arrangement of adjacent [VO_6] octahedra sharing edges to form a hexagonal close-packed lattice with considerable V−V overlap, *i.e.* the V−V1 bonds in Fig.6(b). And below the transition temperature, a small distortion of the [VO_6] octahedra yields alternate long and short V−V bonds to form pairs of V atoms in VO_2(M), *i.e.* the V−V1 and V−V2 bonds in Fig.6(a), leading to the semiconducting behavior [32].

The grain size is widely believed to determine the MIT temperature and hysteresis width of VO_2(M) [4, 24−26]. The ascription of the MIT at low temperature

DOI:10.1063/1674-0068/27/04/471-474

to pure size effect can be excluded, because it has been proven that the MIT temperature decreased with decreasing size in the VO_2(M) nanoparticles [27], and the MIT temperature increased while the hysteresis width decreased when the size of VO_2(M) nanocrystals decreased from 30 nm to 10 nm [28]. It was found that the oxygen vacancy can tune the MIT temperature in a wide range [29], and the MIT of VO_2(M) beam can be achieved at room temperature by active control of strain [30]. Our recent results also indicated that the MIT temperature of VO_2(M) nanoparticles can be regulated by size- and defect-effect [31], and the defect-effect is the main contribution to the regulation of the MIT temperature at low temperature. These results clearly indicate that the MIT temperature and the hysteresis width strongly depend on the internal structure and lattice distortion of VO_2(M), and the MIT at low temperature mainly comes from the strain effect besides the size effect.

IV. CONCLUSION

In this work, VO_2(B) nanorods gradually transform to VO_2(M) nanorods with increasing annealing temperature, and pure VO_2(M) nanorods can be obtained upon annealing treatment at 550 °C. There are two pairs of the endothermic and exothermic peaks (two MITs) in the mixed phase of VO_2(B) and VO_2(M), one is at low temperature between −3 and 19 °C, and the other is at high temperature of 65−74 °C. The low temperature MIT is closely associated with the VO_2(M) grains in the strain environment of VO_2(B) nanorods instead of pure size effect, and that at high temperature side origins from bulk VO_2(M) nanorods.

V. ACKNOWLEDGMENTS

This work was financially supported by the National Natural Science Foundation of China (No.51372250).

[1] F. J. Morin, Phys. Rev. Lett. **3**, 34 (1959).
[2] C. Leroux, G. Nihoul, and G. Van Tendeloo, Phys. Rev. B **57**, 5111 (1998).
[3] M. M. Qazilbash, M. Brehm, B. G. Chae, P. C. Ho, G. O. Andreev, B. J. Kim, S. J. Yun, A. V. Balatsky, M. B. Maple, and F. Keilmann, Science **318**, 1750 (2007).
[4] L. Whittaker, C. Jaye, Z. Fu, D. A. Fischer, and S. Banerjee, J. Am. Chem. Soc. **131**, 8884 (2009).
[5] G. L. Petrov, V. V. Yakovlev, and J. Squier, Appl. Phys. Lett. **81**, 1023 (2002).
[6] C. Z. Wu, F. Feng, and Y. Xie, Chem. Soc. Rev. **42**, 5157 (2013).
[7] L. Whittaker, H. Zhang, and S. Banerjee, J. Mater. Chem. **19**, 2968 (2009).
[8] J. Zou, Y. G. Peng, and H. Lin, J. Mater. Chem. A **1**, 4250 (2013).
[9] G. P. Nagabhushana and G. T. Chandrappa, J. Mater. Chem. A **1**, 11539 (2013).
[10] Z. F. Peng, W. Jiang, and H. Liu, J. Phys. Chem. C **111**, 1119 (2007).
[11] F. Y. Kong, M. Li, S. S. Pan, Y. X. Zhang, and G. H. Li, Mater. Res. Bull. **46**, 2100 (2011).
[12] C. M. Zheng, X. M. Zhang, J. H. Zhang, and K. R. Liao, J. Solid State Chem. **156**, 274 (2001).
[13] J. H. Son, J. Wei, D. Cobden, G. Z. Cao, and Y. N. Xia, Chem. Mater. **22**, 3043 (2010).
[14] C. Wu, X. Zhang, J. Dai, J. Yang, Z. Wu, S. Wei, and Y. Xie, J. Mater. Chem. **21**, 4509 (2011).
[15] W. Chen, J. F. Peng, L. Q. Mai, H. Yu, and Y. Y. Qi, Solid State Commun. **132**, 513 (2004).
[16] D. Alie, L. Gedvilas, Z. W. Wang, R. Tenent, C. Engtrakul, Y. F. Yan, S. E. Shaheen, A. C. Dillon, and C. M. Ban, J. Solid State Chem. **212**, 237 (2014).
[17] S. D. Ji, F. Zhang, and P. Jin, J. Solid State Chem. **184**, 2285 (2011).
[18] R. Lopez, T. E. Haynes, L. A. Boatner, L. C. Feldman, and R. F. Jr. Haglund, Phys. Rev. B **65**, 224113 (2002).
[19] E. U. Donev, R. Lopez, L. C. Feldman, and R. F. Jr. Haglund, Nano Lett. **9**, 702 (2009).
[20] J. I. Sohn, H. J. Joo, A. E. Porter, C. J. Choi, K. Kim, D. J. Kang, and M. E. Welland, Nano Lett. **7**, 1570 (2007).
[21] A. Frenzel, M. M. Qazilbash, M. Brehm, B. G. Chae, B. J. Kim, H. T. Kim, A. V. Balatsky, F. Keilmann, and D. N. Basov, Phys. Rev. B **80**, 115115 (2009).
[22] Z. Yang, C. Ko, and S. Ramanathan, J. Appl. Phys. **108**, 073708 (2010).
[23] L. Whittaker, C. J. Patridge, and S. Banerjee, J. Phys. Chem. Lett. **2**, 745 (2011).
[24] K. Appavoo and R. F. Jr. Haglund, Nano Lett. **11**, 1025 (2011).
[25] J. M. Baik, M. H. Kim, C. Larson, A. M. Wodtke, and M. Moskovits, J. Phys. Chem. C **112**, 13328 (2008).
[26] R. Lopez, L. A. Boatner, T. E. Haynes, R. F. Haglund, and L. C. Feldman, Appl. Phys. Lett. **79**, 3161 (2001).
[27] R. Lopez, L. C. Feldman, and R. F. Jr. Haglund, Phys. Rev. Lett. **93**, 177403 (2004).
[28] Y. F. Sun, S. S. Jiang, W. T. Bi, R. Long, X. G. Tan, C. Z. Wu, S. Q. Wei, and Y. Xie, Nanoscale **3**, 4394 (2011).
[29] J. Jeong, N. Aetukuri, T. Graf, T. D. Schladt, M. G. Samant, and S. S. P. Parkin, Science **339**, 1402 (2013).
[30] J. Cao, E. Ertekin, V. Srinivasan, W. Fan, S. Huang, H. Zheng, J. W. L. Yim, D. R. Khanal, D. F. Ogletree, J. C. Grossman, and J. Wu, Nature Nanotech. **4**, 732 (2009).
[31] M. Li, X. Wu, L. Li, Y. X. Wang, D. B. Li, J. Pan, S. J. Li, L. T. Sun, and G. H. Li, J. Mater. Chem. A **2**, 4520 (2014).
[32] J. B. Goodenough, J. Solid State Chem. **3**, 490 (1971).

DOI:10.1063/1674-0068/27/04/471-474